



New strategy for fabricating Cd(II) sensing electrochemical interface based on enhanced adsorption followed by redox processes: Ferro-cerium oxide nanocomposite as an example

Kang-Ping Cui ^a, Ru-Ru Dai ^{a,b}, Xu Liu ^{a,b}, Rohan Weerasooriya ^{b,c}, Zhan-Yong Hong ^b, Xing Chen ^{a,b,d,*}, Yu-Cheng Wu ^{b,d}

^a School of Resources and Environmental Engineering, Hefei University of Technology, Hefei, 230009, PR China

^b Key Lab of Aerospace Structural Parts Forming Technology and Equipment of Anhui Province, Institute of Industry and Equipment Technology, Hefei University of Technology, Hefei, 230009, PR China

^c National Institute of Fundamental Studies, Kandy, 20000, Sri Lanka

^d School of Materials Science and Engineering, Hefei University of Technology, Hefei, 230009, PR China



ARTICLE INFO

Article history:

Received 21 November 2019

Received in revised form

12 February 2020

Accepted 26 February 2020

Available online 29 February 2020

Keywords:

Ferro-cerium oxide

Nanocomposite

Sol-gel combustion method

Cadmium ions

Square wave anode stripping voltammetry

ABSTRACT

Cd(II) is a biologically active element that requires rapid and reliable monitoring for its pollution control. We designed the electrochemical sensing nanocomposite with enhanced adsorption followed by redox processes, which was synthesized by incorporating ferric ions into cerium oxide substrate (hereafter CeFe₂O₅) via the sol-gel combustion method. The CeFe₂O₅ nanocomposite modified glassy carbon electrode (CeFe₂O₅/GCE) was used for selective detection of Cd(II) by square wave anode stripping voltammetry (SWASV). At optimal experimental conditions, the observed sensitivity and detection limits of CeFe₂O₅/GCE are 31.68 μA/μM and 0.94 nM, respectively. Our CeFe₂O₅/GCE exhibits excellent stability (RSD 3.34%) and analytical precision for Cd(II). The CeFe₂O₅/GCE can also be used in trace detection of heavy metal ions spiked in environmental samples. The nanocomposites with high electrochemical performance would be of great interest for constructing novel sensing platforms for monitoring heavy metal ions in environment.

© 2020 Elsevier B.V. All rights reserved.

1. Introduction

Cadmium is a carcinogenic metal ion ubiquitous in the environment due to industrial and agricultural activities [1,2]. Most of the accumulated cadmium in biological tissues routed through food, and the World Health Organization (WHO) listed it as a priority pollutant. The WHO maximum contaminant goal limits for cadmium(II) is 27 nM for drinking waters. Excess Cd(II) accumulates in kidneys and liver of the human body implicating various health disorders. Cd(II) readily exchanges with Ca(II) in bones, which results in them weakening to cause *itai itai* disease [3,4]. The development of a rapid and robust detection method for Cd(II) in food and water is, therefore, listed as a priority.

To date, several robust, sensitive and reliable methods as

inductively coupled plasma mass spectrometry (ICP-MS) [5], inductively coupled plasma optical emission spectrometry (ICP-OES) [6], fluorescence spectrometry [7], atomic emission spectroscopy (AES) [8], atomic absorption spectroscopy (AAS) [9] are widely used for the detection of total cadmium in various sample matrixes. However, the methods mentioned above suffer from the inability of in situ chemical speciation measurements, skilled operational/maintenance labor, capital cost, and non-portability in the field. In contrast, electrochemical detection methods have advantages with High detection speed, sensitivity, simple operation and selectivity, and in situ chemical species detection. Although potentiometric Cd(II) ion-selective electrode sensors able to measure free Cd²⁺ in solution, their low detection limits are around 1 μM restrict applicability in environmental measurements. Out of anode stripping voltammetric methods, square wave anode stripping voltammetry (SWASV) is widely used for trace detection of heavy metal ions because of its enhanced sensitivity, selectivity, stability, and minimal interfering from dissolved reactive gases as oxygen abundant in the environment [10].

* Corresponding author. School of Resources and Environmental Engineering, Hefei University of Technology, Hefei, 230009, PR China.

E-mail address: xingchen@hfut.edu.cn (X. Chen).

The active layer of the sensing probe can engineer to achieve desired functionalities, and we modified it to yield high selective Cd(II) detection with enhanced sensitivity [11]. Metal oxide nanocomposites such as MnCo₂O₄ [12], Fe₂O₃/graphene [13], MnFe₂O₄ [15] hold a great promise in the fabrication of modified electrochemical sensors for Cd(II) detection in the presence of other metal ions. They mainly focus on the improvement of the adsorption properties of sensing interface towards the target heavy metal ions, and little attention was laid on facilitating redox reactions on the electrochemical sensing interfaces.

We have selected CeO₂ derived nanocomposite to fabricate Cd(II) electrochemical sensor due to the following reasons: a. CeO₂ enriches with high defect density in a controllable fashion [14,15]; b. Foreign metal ions form solid solutions with CeO₂, and the properties of the composite can be engineered [16]; c. The migration of gases within the solid can modulate with carefully designed CeO₂ composites [17]. Herein, we doped CeO₂ by Fe³⁺ to fabricate Cd(II) selectively sensing nanocomposite. The defects of poor conductivity in CeO₂ were healed by Fe³⁺ citrate chelation. The high sorption on Fe₂O₃ for Cd(II) was used to arrest the metal ion on the active layer for its fast responses. Further, Fe³⁺-doped CeO₂ substrate facilitates electron transfer Cd(II)→Cd(0) conversion, and the sensitivity of the probe can be further enhanced. The nanocomposite modified glassy carbon electrode was used for selective detection of Cd(II) by square wave anode stripping voltammetry (SWASV) method. To demonstrate its potential applications, the spiked Cd(II) in natural water samples were also been detected with the as-fabricated electrochemical sensor.

2. Experimental

2.1. Chemicals and reagents

Required analytical grade chemicals were obtained from Shanghai Chemical Reagent Co. LTD, China, and were used as received. Supporting electrolyte buffers were prepared as follows: of 0.1 M acetate buffer using 0.1 M NaAC and 0.1 M HAC, 0.1 M phosphate buffer (PBS) using 0.1 M KH₂PO₄ and 0.1 M Na₂HPO₄, 0.1 M citrate buffer using 0.1 M citric acid and 0.1 M sodium citrate. Sol-gel combustion method was used to synthesize CeFe₂O₅ using Fe(NO₃)₃·9H₂O and CeCl₃·7H₂O. Ultrapure water (18.2 MΩ cm) water was used for all reagent preparations (HK-UP-10 ultra-pure water).

2.2. Apparatus

Cyclic voltammetry (CV), electrochemical impedance spectroscopy (EIS) and square wave anode stripping voltammetry (SWASV) determinations were carried out by high precision electrochemical workstation (CHI760E). The three-electrode system is used with bare glassy carbon electrode (GCE) or modified GCE as a working electrode; Ag/AgCl/KCl_{saturated} electrode as a reference electrode and Pt counter electrode. Scanning electron microscopy (SEM) was carried out on CeFe₂O₅. The phase structure and phase purity were examined by X-ray diffraction (XRD, XPert PRO MPD) in the 2θ range from 5° to 70° with Cu-K_α radiation ($\lambda = 1.5418 \text{ \AA}$). The iron and cerium elemental analysis was carried out using inductively coupled plasma mass spectrometry (ICP-MS, Agilent7500).

2.3. Preparation of nanostructured CeFe₂O₅ composite

Nanostructured composite oxides were prepared by the sol-gel combustion method using iron(III) and cerium(IV) salts [18]. The ratio of Fe(III): Ce(IV) of nanocomposites was controlled, adding different proportions of CeCl₃·7H₂O. For the preparation of CeFe₂O₅

nanocomposite was synthesized as given below: 0.04 mol Fe (NO₃)₃·9H₂O and 0.02 mol CeCl₃·7H₂O were added to 200 ml deionized water and the mixture was stirred for 2 h at 60 °C. Then 0.06 mol citric acid was added to the mixture, and stirring was continued for 2 h at 60 °C. Then the solution was dried in an oven at 125 °C for 12 h. The nitrate-citric acid gel thus resulted was calcined for 2 h at 400 °C to yield CeFe₂O₅ nanocomposite.

2.4. Preparation of modified GCE

The surface of the GCE was polished with aluminum oxide powder of 1.0 μM, 0.3 μM, and 0.05 μM grain sizes to yield a shiny surface. Then the glassy carbon electrode was ultra-sonicated in 1:1 (V: V) HNO₃, absolute ethyl alcohol, and deionized water successively for 2 min. The GCE was dried at room temperature. Then 3 mg CeFe₂O₅ deliquesced in 3 ml deionized aqueous solution and homogenized by ultra-sonication for 30 min. The 5 μL of the suspension was dropped onto the freshly polished GCE surface and dried in a nitrogen atmosphere. As controls, GCEs modified with Fe₂O₃ or CeO₂ were prepared similarly. The surface of all modifications GCE required polishing before repeated measurements were carried out.

3. Results and discussions

3.1. Characterization of CeFe₂O₅ nanocomposite

The SEM images of CeFe₂O₅ nanocomposite (Fig. 1a), Fe₂O₃, and CeO₂ (Fig. S1) are obtained. The CeFe₂O₅ possesses homogeneous smooth-surfaced grains of around 100–200 nm diameter with rounded edges (Fig. 1a). The elemental composition of CeFe₂O₅ was determined by ICP-MS (Table S1). The measured and theoretical Fe: Ce molar ratio of our composite and CeFe₂O₅ agrees well within experiment errors, and the data support CeFe₂O₅ formation. The XRD data trends represent a well-crystallized CeFe₂O₅ composite (Fig. 1b). The XRD peaks at 2θ = 24.18°, 33.18°, 35.74°, 40.92°, and 54.1°, are ascribed to (110), (121), (−110), (120), and (132) planes of Fe₂O₃ in CeFe₂O₅, respectively (JCPDS File No.85-0987-Fe₂O₃). The secondary peaks at 28.7°, 47.54°, 56.5°, and 59.32°, are ascribed to (111), (220), (311) and (222) planes of CeO₂ in CeFe₂O₅ phase respectively (JCPDS File No.75-0076-CeO₂) [19–21]. The development of crystallographic planes of our CeFe₂O₅ confirms the presence of distinct planes, as shown in SEM images.

The XPS survey spectrum of CeFe₂O₅ was obtained in 1300 to 0 eV range (Fig. 2a), and high-resolution spectrums for Ce, Fe, and O are also shown (Fig. 2b, 2c, 2d). The XPS peaks at 901.2 eV and 882.51 eV corresponds to the presence of Ce 3d_{3/2} and Ce 3d_{5/2} chemical states, respectively. The presence of Fe 2p_{1/2} and Fe 2p_{3/2} chemical states is confirmed by 724.29 eV and 710.37 eV XPS peaks (Fig. 2c). The observed binding energies are following trivalent state iron, and it, therefore, confirms CeFe₂O₅ nanocomposite [22]. Fig. 2b shows that, the Ce 3d peaks at 882.51 eV, 898.39 eV and 916.83 eV are due to Ce(IV) oxide species [22]. The binding energy of oxygen in CeFe₂O₅ is 529.62 eV, demonstrating a slight shift from 529.2 eV observed in other metal oxides, which might be due to synergy between Ce—O and Fe—O [23].

3.2. Voltammetric behaviors of different modified electrodes

Cyclic voltammetry (CV) and electrochemical impedance spectroscopy (EIS) methods are used to characterize the electrons transfer behavior of electrode-solution interface [24,25]. We used CV and EIS measurements to characterize charge transfer of bare and modified GCEs using 5 mM [Fe(CN)₆]^{3-/4-} redox probing solution in 0.1 M KCl (Fig. 3a, 3b) [26]. When compared to bare GCE, due to poor

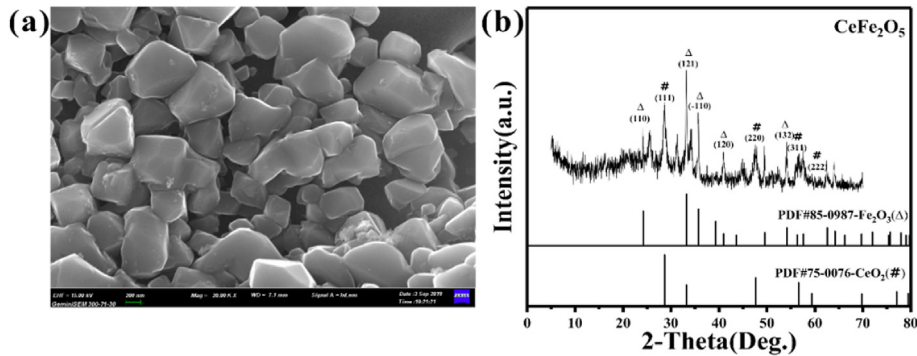


Fig. 1. (a) SEM images of CeFe₂O₅; (b) XRD patterns of CeFe₂O₅.

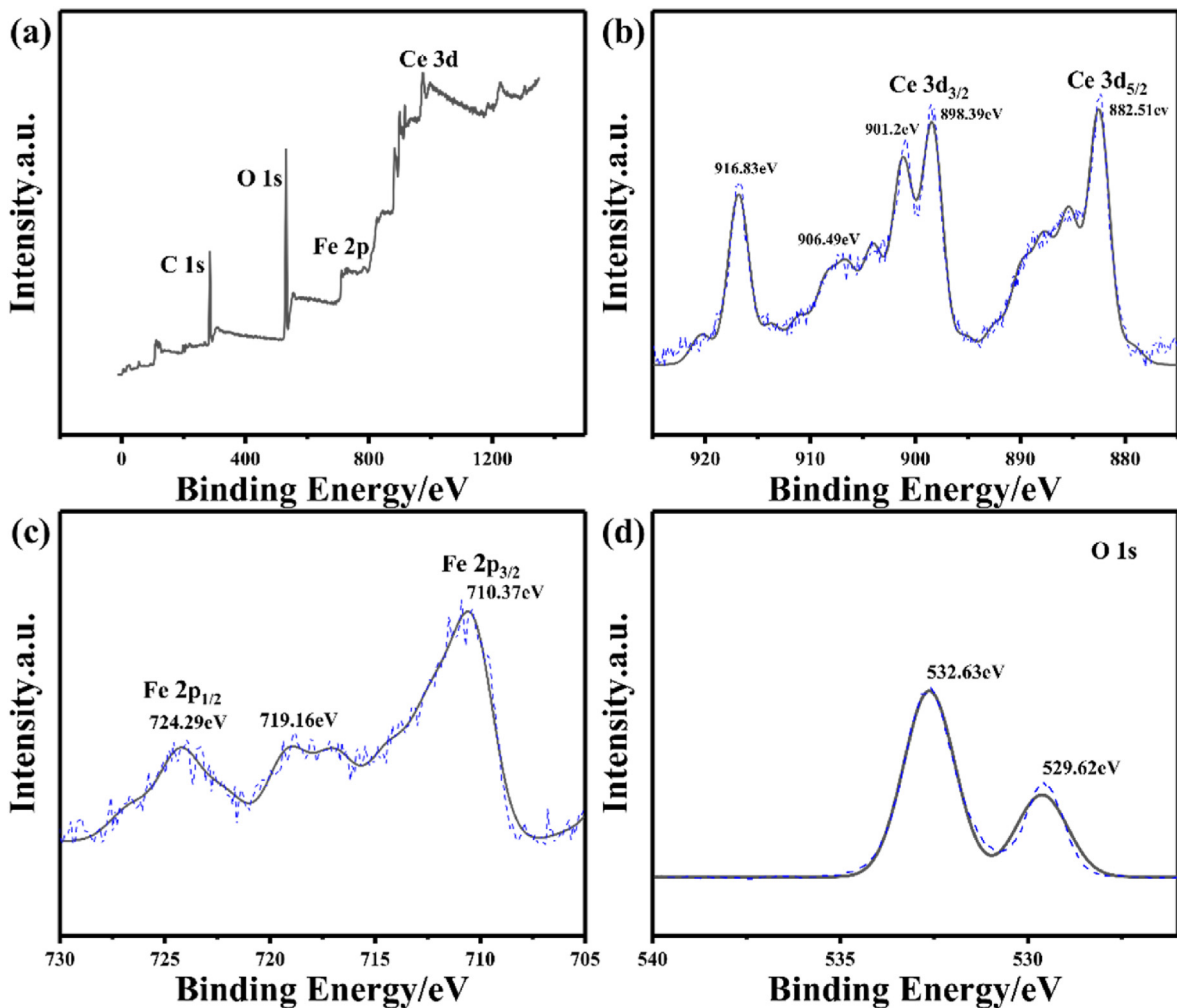


Fig. 2. XPS spectra of CeFe₂O₅. (a) XPS survey spectrum; High resolution of Ce 3d (b), Fe 2p (c), and O 1s (d) spectra.

conductivity of CeO₂ or Fe₂O₃, the anodic and cathodic peak currents measured in the redox probing solution with Fe₂O₃/GCE or CeO₂/GCE decreases rapidly with a large peak to peak separation [27]. The anodic and cathodic peak currents of CeFe₂O₅/GCE increase compared to CeO₂/GCE and Fe₂O₃/GCE, due to enhanced electrochemical conductivity of iron and cerium oxide composites [28].

The performance of charge transfer at the electrode-solution interface was further examined by EIS (Fig. 3b). In the EIS spectra, the semi-circle represents limiting the nature of charge transfer, and

the diameter measures equivalent charge transfer resistance (R_{eq}). When the diameter increases, the R_{ret} also increases inhibiting electrons transfer [29]. When compared to bare GCE, CeO₂, and Fe₂O₃ modified GCE, the reduced R_{ret} value of CeFe₂O₅ modified GCE implies enhanced electron transfer rates of CeFe₂O₅ nanocomposites. The observations are consistent with the CV results [30].

Electrochemical performance of Fe₂O₃, CeO₂, or CeFe₂O₅ modified GCE for Cd(II) detection was examined by SWASV method using 0.8 μM Cd²⁺ in 0.1 M PBS at pH 5.0. The deposition potential

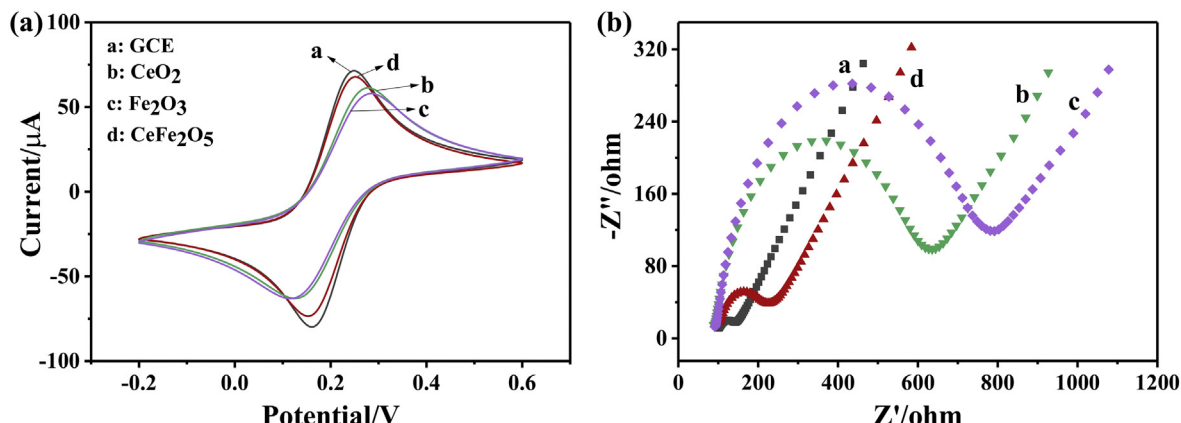


Fig. 3. (a) Cyclic Voltammograms of bare, CeO₂, Fe₂O₃, and CeFe₂O₅ modified GCE. (b) Nyquist electrochemical impedance spectra for bare, CeO₂, Fe₂O₃, and CeFe₂O₅ modified GCE in 5 mM Fe(CN)₆^{3-/4-} with 0.1 M KCl.

and time were kept at -1.3 V and 120 s, respectively, and the results thus obtained are shown in Fig. 4. The Cd(II) detection by Fe₂O₃ or CeO₂ modified GCE is poor. Practically no measurable current responses were seen. However, peaks at -0.5 V (Fe₂O₃/GCE) or -0.9 V (CeO₂/GCE) is ascribed due to other redox processes that required detailed investigation. When compared to bare GCE, the CeFe₂O₅/GCE shows superior detection currents for Cd(II). When Fe³⁺ concentration in the solid is high, the oxygen vacancy concentration is reduced or becomes zero resulting in poor detectability for Cd(II) (Fig. S2) [31]. Optimal Cd(II) response current appeared with CeFe₂O₅ GCE at Ce: Fe 1:2 ratio. We used CeFe₂O₅/GCE for further analysis of this work.

3.3. Optimization of experimental conditions

The Cd²⁺ detection by CeFe₂O₅/GCE was optimized for the following parameters: electrolyte type, pH, deposition potential, and deposition time. Optimization of these parameters helps to zoom out the potential window and hydrolysis of metal ions [32].

The effect of electrolyte type for Cd²⁺ detection by CeFe₂O₅/GCE was evaluated using three buffers at pH 5.0, -1.0 V deposition potential, and 120 s deposition time (Fig. 5a). The electrolyte type

exerts a significant effect on the response current. The highest response current for Cd²⁺ detection was observed in 0.1 M PBS buffer, and hence it was used for other experiments. The effect of pH on the Cd²⁺ response current was examined from pH 5.0 to 8.0 (Fig. 5b). When pH < 5.0 , the PBS buffer requires acid addition to regulate pH. Hence, our experiments confined to pH 5.0–8.0. The depositional potential and time were -1.0 V and 120 s, respectively. The response current for Cd²⁺ is the highest at pH 5.0. When pH < 5.0 , cadmium occurs as free Cd²⁺. When the pH increased, the activity of the free Cd²⁺ at the expense of forming Cd(OH)_x species, and therefore the response current sow gradual decrease. Hence, 0.1 M PBS buffer with pH = 5.0 was selected as the supporting electrolyte for further experimental measurement.

The deposition potential is also an important parameter affecting the sensitivity of the electrochemical sensor (Fig. 5c). In 0.1 M PBS buffer (pH = 5.0), different deposition potentials were used to obtain the relationship between the peak current and the deposition potential for 0.8 μM Cd²⁺. When the deposition potential changes from -1.4 V to -0.8 V, the peak current of the CeFe₂O₅/GCE for Cd²⁺ detection increases reaching an optimal at -1.4 V. Below, this potential gas bubbles observed on the electrode surface and the response current growth slows down. Therefore, we chose -1.3 V as the optimal deposition potential for subsequent experiments. To obtain optimal deposition time for better detection limits, we selected different deposition times of the 60 s, 90 s, 120 s, 150 s, and 180 s in 0.1 M PBS buffer (pH = 5.0) at -1.3 V deposition potential (Fig. 5d). Additionally, the deposition potential was -1.3 V. Peak current shows an optimal value at 120 s deposition time. The longer the deposition time, the larger the peak current.

3.4. Electrochemical detection of Cd(II) by CeFe₂O₅/GCE

Using the optimized data received from previous experiments for Cd²⁺ detection by SWASV was used with CeFe₂O₅/GCE to determine method sensitivity and detection limits (see Fig. 6). The calibration curve constructed for Cd²⁺) from 0.05 μM to 1.0 μM is linear with $I(\mu\text{A}) = -8.4 + 31.68 C(\mu\text{M})$, $R^2 = 0.994$. Under optimal conditions determined previously, Cd²⁺ was detected by SWASV on the CeFe₂O₅/GCE. The sensitivity and the detection limit of the method are 0.94 nM and 31.68 μA/μM, respectively.

Table 1 shows the sensitivity and detection limits of our data in comparison with published data for other modified electrodes. As well as the electrochemical sensing values of Cd²⁺ previously measured on various other modified electrodes. We obtain the highest sensitivity and detection limits with CeFe₂O₅/GCE for Cd²⁺

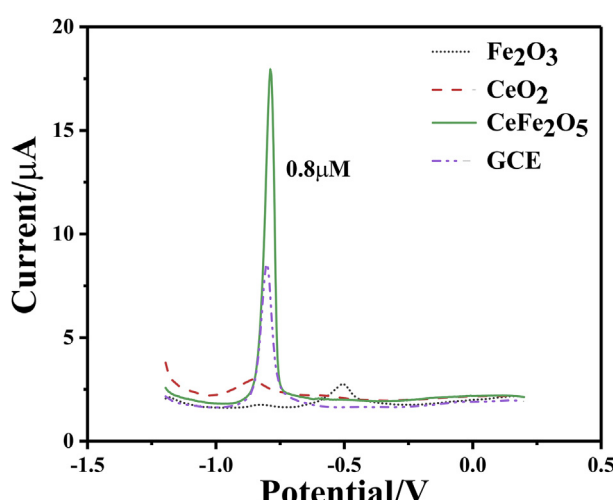


Fig. 4. SWASV responses for 0.8 μM Cd²⁺ on different modified electrodes in 0.1 M PBS (pH 5.0). Under the following conditions: deposition potential -1.3 V, accumulation time 150 s, step potential 5 mV, amplitude 25 mV, frequency 15 Hz.

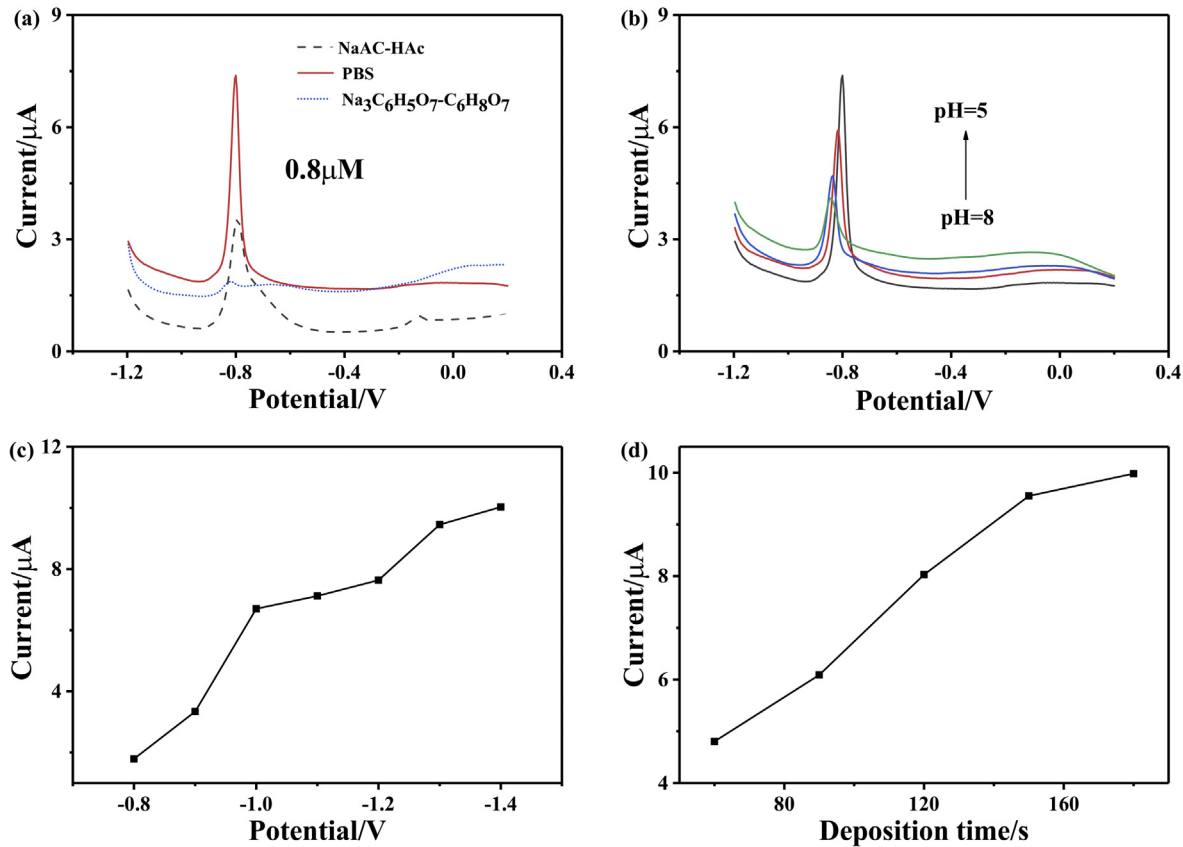


Fig. 5. (a) SWASV responses for $0.8 \mu\text{M}$ Cd^{2+} in 0.1 M different buffer solution (pH 5.0). Under the conditions: deposition potential -1.0 V , accumulation time 120 s ; (b) SWASV responses for $0.8 \mu\text{M}$ Cd^{2+} at different pH value in PBS (pH 5.0). Under the conditions: deposition potential -1.0 V , accumulation time 120 s ; (c) SWASV responses for $0.8 \mu\text{M}$ Cd^{2+} at different deposition potential in 0.1 M PBS (pH 5.0). Under the conditions: accumulation time 120 s ; (d) SWASV responses for $0.5 \mu\text{M}$ Cd^{2+} at different accumulation times in 0.1 M PBS (pH 5.0). Under the conditions deposition potential of -1.3 V .

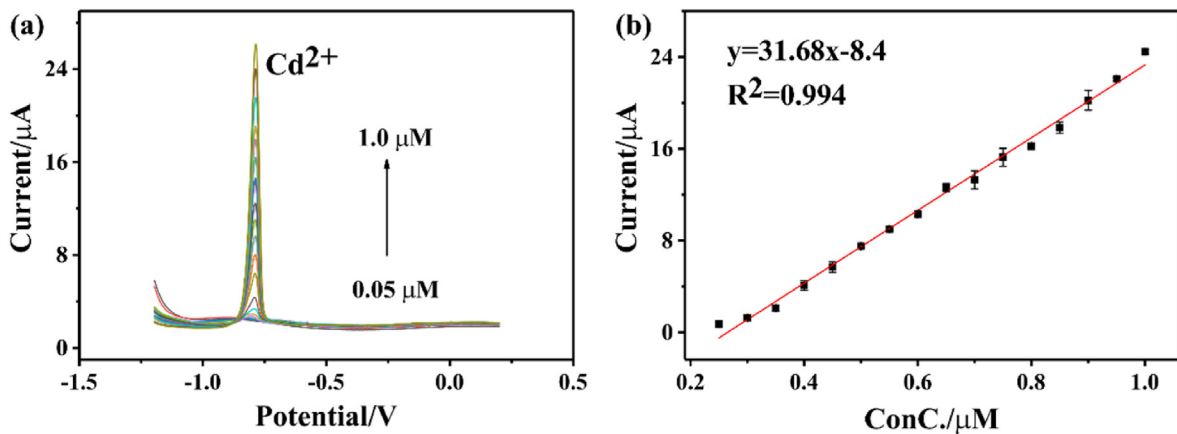


Fig. 6. (a) SWASV response of the $\text{CeFe}_2\text{O}_5/\text{GCE}$ for the analysis of Cd^{2+} over a concentration range of $0.05 \mu\text{M}$ – $1.0 \mu\text{M}$; (b) Corresponding linear calibration of peak current.

detection, and the performance of the new sensor exceeds current method guidelines set by the WHO drinking water standards [40]. During the pre-enrichment process, Cd^{2+} is adsorbed onto the surface of CeFe_2O_5 and then released to the electrode surface for deposition and stripping. The combination of iron and cerium oxide enhanced the adsorption capacity of Cd^{2+} . Moreover, the high specific surface area of nanocomposite facilitates for Cd^{2+} to diffuse and accumulate on the sensor. Herein, the CeFe_2O_5 nanocomposite seems conduit of electron transfer, reaching enhanced response current for Cd^{2+} .

3.5. Chemical interference by other metal ions

We examined the chemical interference by Cu^{2+} , Hg^{2+} , and Pb^{2+} on Cd^{2+} by $\text{CeFe}_2\text{O}_5/\text{GCE}$. The concentration of the matrix metal ions was kept at $0.5 \mu\text{M}$ while Cd^{2+} was varied $0.2 \mu\text{M}$ – $0.7 \mu\text{M}$. Single-mode, e.g., Cd^{2+} vs. matrix cation, or multimode, e.g., Cd^{2+} vs. all matrix cations, was conducted, and the data are shown in Fig. 7. The response peaks of Cu^{2+} and Hg^{2+} appear at -0.124 V and $+0.236 \text{ V}$, respectively [41]. However, we could not obtain a

Table 1Comparison of current sensitivity with previously reported values of different electrodes for electrochemical detection of Cd^{2+} .

Electrode	Linear range (μM)	LOD (μM)	Sensitivity ($\mu\text{A}/\mu\text{M}$)	Ref
rGO-Fe ₃ O ₄ /GCE	0.4–0.8	0.056	14.82	[33]
Fe ₃ O ₄ /CPE	0.01–35.6	0.047	0.038	[34]
SnO ₂ Tube-in-Tube/GCE	0.2–1.4	0.1	12.88	[35]
MnFe ₂ O ₄ @Cys GCE	0.4–1.5	0.0632	9.31	[36]
Fe ₃ O ₄ -chitosan/GCE	1.2–1.7	0.0392	8.11	[37]
Fe ₃ O ₄ /GCE	0.1–2.0	0.156	6.0	[38]
NH ₂ -MIL-88(Fe)-rGO/GCE	0.005–0.3	0.0049	190.36	[39]
CeFe ₂ O ₅ /GCE	0.05–1.0	0.00094	31.68	This work

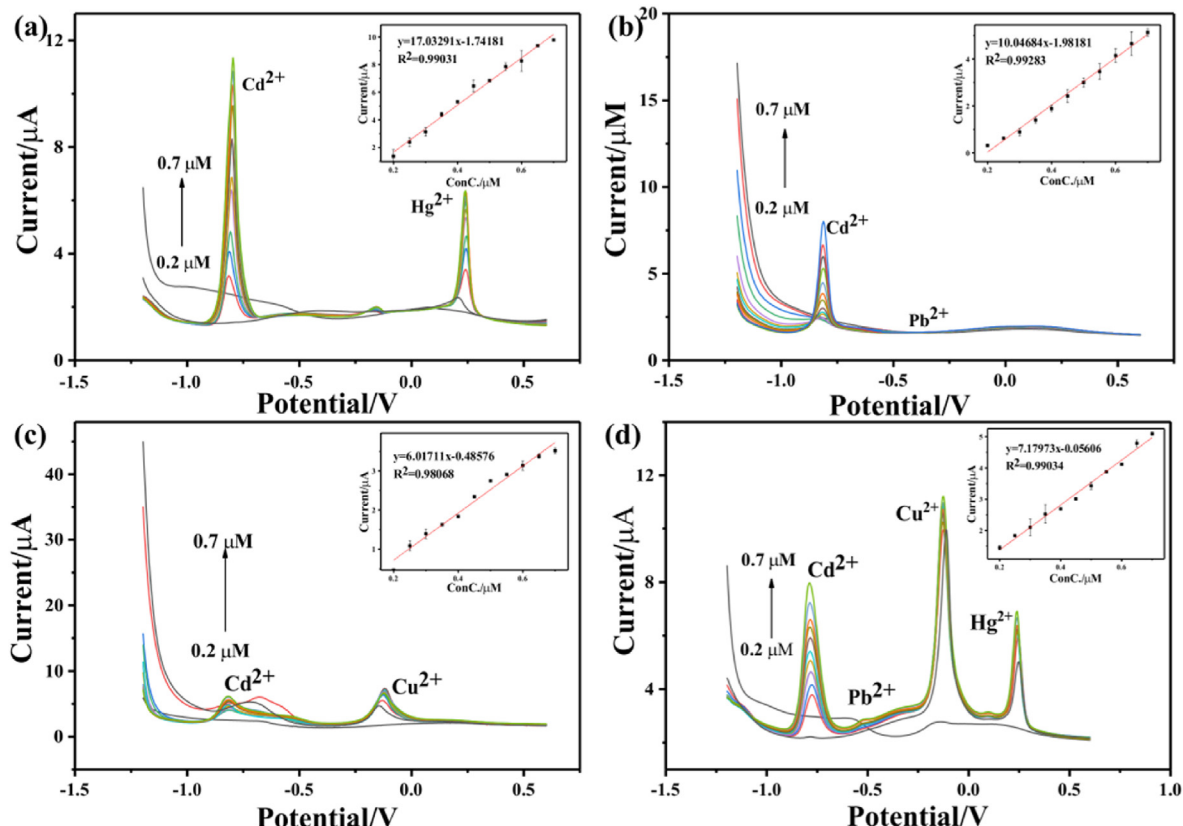
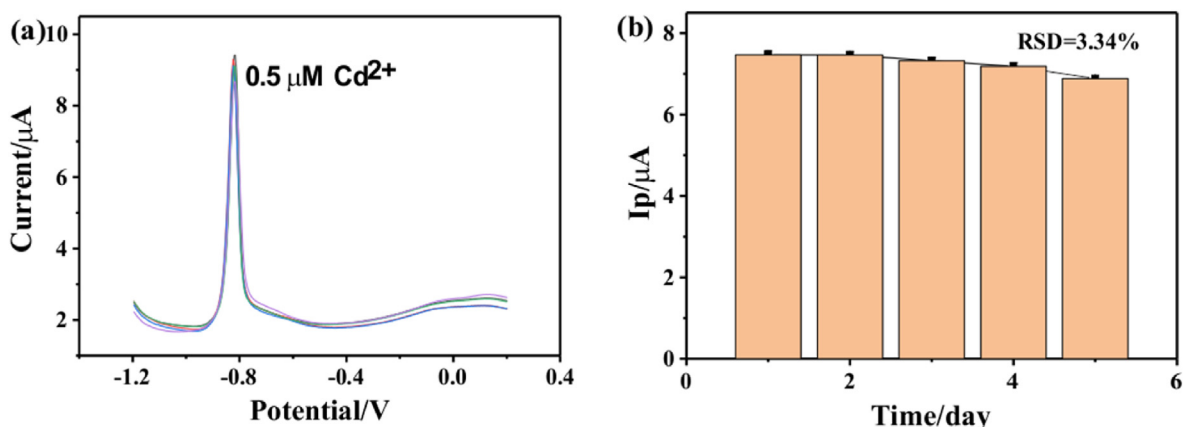
**Fig. 7.** SWASV response of the CeFe₂O₅ modified electrode toward Cd²⁺ over a concentration range of 0.2 μM –0.7 μM when adding (a) 0.5 μM Hg²⁺, (b) 0.5 μM Pb²⁺, (c) 0.5 μM Cu²⁺, and (d) 0.5 μM Hg²⁺, Pb²⁺ and Cu²⁺, respectively.**Fig. 8.** The repetitive toward 0.5 μM Cd²⁺ after stored at room temperature for 5 days under optimized conditions in 0.1 M PBS solution.

Table 2Determination of spiked Cd²⁺ in real samples (number of samples assayed = 3).

Samples	Cd ²⁺ added (μM)	Cd ²⁺ found (μM)	RSD (%)	Recovery (%)
Sample I	0.3	0.308	3.6	102.7
	0.5	0.498	4.8	99.6
	0.8	0.769	1.1	96.1
Sample II	0.3	0.307	1.7	102.3
	0.5	0.501	2.6	100.2
	0.8	0.762	1.5	95.3

peak for Pb²⁺ by CeFe₂O₅/GCE. Herein, the sensitivity of Cd²⁺ reduced markedly due to competing effect for restricted sites on the electrode surface [37]. In single element mode, the addition of Cd²⁺, the peaks of Cu²⁺ and Hg²⁺ exist in different proportions. When Hg²⁺ exists, which may be due to the formation of mercury film on the electrode surface during the deposition, reducing the sensitivity of Cd²⁺ [40]. When Cu²⁺ is present, the sensitivity of Cd²⁺ reduced mostly. The interference between Cd²⁺ and Cu²⁺ may vary due to the substitution of Cu²⁺ for Cd²⁺ during the pre-concentration [42]. In multi-element mode, the Cd²⁺ detection is reduced in the presence of Cu²⁺, Hg²⁺, and Pb²⁺. When Pb²⁺, Hg²⁺, Cu²⁺, and Cd²⁺ were measured at the same time, although there were mutual interferences, except Pb²⁺, the peaks of Hg²⁺, Cu²⁺ and Cd²⁺ are well separated. Therefore, CeFe₂O₅/GCE can still be used for the simultaneous determination of four target ions with acceptable anti-interference capability [43].

3.6. Regenerative evaluation

To evaluate the reproducibility of the CeFe₂O₅/GCE, we repeated the Cd²⁺ measurements both in single-element and multi-element modes for five consecutive days, and the CeFe₂O₅ modified glassy carbon electrode was adopted to detect the solution of 0.5 μM Cd²⁺ in 0.1 M PBS (pH = 5.0). The peak current of Cd²⁺ was almost unchanged compared to the newly modified electrode (relative standard deviation (RSD): 3.3%, shown in Fig. 8). We concluded that our CeFe₂O₅/GCE showed excellent reproducibility for detection Cd²⁺.

3.7. Natural water sample analysis

We collected two natural water samples of different dates from the Hubing Lake in Hefei University of Technology for chemical analysis of Cd²⁺ using CeFe₂O₅/GCE by SWASV. The conventional characterization results of the two samples were listed in Table S2. Before the electrochemical detection, the sample was diluted at a 1:9 ratio in 0.1 M PBS buffer (pH = 5). We cannot obtain a response signal for Cd²⁺, indicating that there is no Cd²⁺ contamination in the water. Then, the diluted lake water samples were spiked with Cd²⁺ at concentrations of 0.3 μM , 0.5 μM , and 0.8 μM . For the spiked Cd²⁺ in two samples, the spike recoveries were 95.3%–102.7%, and the relative standard deviations (RSD) were 1.1% ~ 4.8% (see Table 2). The high spike recoveries and low RSD values show that our method of Cd²⁺ detection can be applied practically in single and multi-element modes [44].

4. Conclusions

We synthesized CeFe₂O₅ by a simple sol-gel method for trace electrochemical detection of Cd²⁺. The CeFe₂O₅/GCE has excellent electrochemical sensing performance with high stability and reproducibility based on the enhanced adsorption followed by redox processes. Under optimal experimental conditions, the

observed sensitivity and detection limit of CeFe₂O₅/GCE are 31.68 $\mu\text{A}/\mu\text{M}$ and 0.94 nM, respectively. The achieved detection limit was far below the WHO recommended limits for Cd(II) regulation (27 nM). And also, the as-fabricated sensors succeeded in detect spiked Cd(II) in natural water samples with a high recovery ratio of 95.3% ~ 102.7%, and low RSD of 1.1% ~ 4.8%. Our new nanocomposite modified GCE can be used to detect Cd(II) in natural water samples with high sensitivity, low cost, and robustness, which would be one of the promising methods for fast screening heavy metal ions in the environment.

Declaration of competing interest

The authors declare that they have no known competing financial interests or personal relationships that could have appeared to influence the work reported in this paper.

CRedit authorship contribution statement

Kang-Ping Cui: Methodology, Validation, Writing - original draft. **Ru-Ru Dai:** Methodology, Validation, Writing - original draft. **Xu Liu:** Methodology, Validation. **Rohan Weerasooriya:** Conceptualization, Writing - review & editing, Supervision. **Zhan-Yong Hong:** Writing - review & editing. **Xing Chen:** Validation, Investigation. **Yu-Cheng Wu:** Funding acquisition.

Acknowledgments

The authors acknowledge the financial support from National Basic Research Program of China (Grant No. SQ2019YFC040023), National Natural Science Foundation of China (Grant No. 21777164), Fundamental Research Funds for the Central Universities (Grant No. PA2019GDQT0019), and Key Technologies R & D Program of Anhui Province (No. 1704c0402195). R. W. acknowledges the Program of Distinguished Professor in B&R Countries (Grant No. DL20180052).

Appendix A. Supplementary data

Supplementary data to this article can be found online at <https://doi.org/10.1016/j.jallcom.2020.154551>.

References

- [1] M.P. Waalkes, Cadmium carcinogenesis in review, *Inorg. Biochem.* 79 (2000) 241–244.
- [2] K. Pyrzynska, Removal of cadmium from wastewaters with low-cost adsorbents, *J. Environ. Chem. Eng.* 7 (2019).
- [3] P. Polykretis, F. Cencetti, C. Donati, E. Luchinat, L. Banci, Cadmium effects on superoxide dismutase 1 in human cells revealed by NMR, *Redox Biol.* 21 (2019) 101102.
- [4] R. Xiong, Q. Wu, R. Trbojevich, L. Muskhelishvili, K. Davis, M. Bryant, P. Richter, X. Cao, Disease-related responses induced by cadmium in an *in vitro* human airway tissue model, *Toxicol. Lett.* 303 (2019) 16–27.
- [5] M. Shen, L. Chen, W. Han, A. Ma, Methods for the determination of heavy metals in indocalamus leaves after different preservation treatment using inductively-coupled plasma mass spectrometry, *Microchem. J.* 139 (2018) 295–300.
- [6] Y. Yamini, M. Safari, Modified magnetic nanoparticles with catechol as a selective sorbent for magnetic solid phase extraction of ultra-trace amounts of heavy metals in water and fruit samples followed by flow injection ICP-OES, *Microchem. J.* 143 (2018) 503–511.
- [7] D. Zhang, W. Jiang, Y. Zhao, Y. Dong, X. Feng, L. Chen, Carbon dots rooted PVDF membrane for fluorescence detection of heavy metal ions, *Appl. Surf. Sci.* 494 (2019) 635–643.
- [8] C. Cerai Ferreira, L. Malta Costa, P.J. Sanches Barbeira, Methyl oleate as matrix simulacrum for the simultaneous determination of metals in biodiesel samples by flame atomic emission spectroscopy, *Talanta* 138 (2015) 8–14.
- [9] V. Kazantzzi, A. Kabir, K.G. Furton, A. Anthemidis, Fabric fiber sorbent extraction for on-line toxic metal determination by atomic absorption spectrometry: determination of lead and cadmium in energy and soft drinks, *Microchem. J.*

- 137 (2018) 285–291.
- [10] B. Tesfaw, S. Mehretie, S. Admassie, Quantification of lead in cooking utensils and vegetables using square wave anodic stripping voltammetry, *Heliyon* 4 (2018), e00523.
- [11] H. Bagheri, A. Afkhami, H. Khosh safar, M. Rezaei, S.J. Sabounchei, M. Sarlakifar, Simultaneous electrochemical sensing of thallium, lead and mercury using a novel ionic liquid/graphene modified electrode, *Anal. Chim. Acta* 870 (2015) 56–66.
- [12] M. Velmurugan, S.M. Chen, Synthesis and characterization of porous MnCo₂O₄ for electrochemical determination of cadmium ions in water samples, *Sci. Rep.* 7 (2017) 653.
- [13] S. Lee, J. Oh, D. Kim, Y. Piao, A sensitive electrochemical sensor using an iron oxide/graphene composite for the simultaneous detection of heavy metal ions, *Talanta* 160 (2016) 528–536.
- [14] S. Afzal, X. Quan, S. Lu, Catalytic performance and an insight into the mechanism of CeO₂ nanocrystals with different exposed facets in catalytic ozonation of p-nitrophenol, *Appl. Catal. B Environ.* 248 (2019) 526–537.
- [15] S.S. Mofarah, E. Adabifiroozjaei, Y. Yao, P. Koshy, S. Lim, R. Webster, X.H. Liu, R.K. Nekouei, C. Cazorla, Z. Liu, Y. Wang, N. Lambopoulos, C.C. Sorrell, Proton-assisted creation of controllable volumetric oxygen vacancies in ultrathin CeO_{2-x} for pseudocapacitive energy storage applications, *Nat. Commun.* 10 (2019).
- [16] Q.Q. Li, Z. Huang, P.F. Guan, R. Su, Q. Cao, Y.M. Chao, W. Shen, J.J. Guo, H.L. Xu, R.C. Che, Simultaneous Ni doping at atom scale in ceria and assembling into well-defined lotuslike structure for enhanced catalytic performance, *Acs Appl Mater Inter* 9 (2017) 16243–16251.
- [17] W. Cai, F. Chen, X. Shen, L. Chen, J. Zhang, Enhanced catalytic degradation of AO₇ in the CeO₂–H₂O₂ system with Fe³⁺ doping, *Appl. Catal. B Environ.* 101 (2010) 160–168.
- [18] J. Li, Y. Ren, F. Ji, B. Lai, Heterogeneous catalytic oxidation for the degradation of p-nitrophenol in aqueous solution by persulfate activated with CuFe₂O₄ magnetic nano-particles, *Chem. Eng. J.* 324 (2017) 63–73.
- [19] Y. Wang, G. Wang, H. Wang, C. Liang, W. Cai, L. Zhang, Chemical-template synthesis of micro/nanoscale magnesium silicate hollow spheres for wastewater treatment, *Chemistry* 16 (2010) 3497–3503.
- [20] S. Thirumalairajan, K. Girija, N.Y. Hebbalkar, D. Mangalaraj, C. Viswanathan, N. Ponpandian, Shape evolution of perovskite LaFeO₃ nanostructures: a systematic investigation of growth mechanism, properties and morphology dependent photocatalytic activities, *RSC Adv.* 3 (2013).
- [21] J.R. Scheffe, M.D. Allendorf, E.N. Coker, B.W. Jacobs, A.H. McDaniel, A.W. Weimer, Hydrogen production via chemical looping redox cycles using atomic layer deposition-synthesized iron oxide and cobalt ferrites, *Chem. Mater.* 23 (2011) 2030–2038.
- [22] Y. Xin, L. Xiaojuan, L. Shangjun, T. Jing, Investigation of enhanced photoelectrochemical property of cerium doped hematite film prepared by sol-gel route, *Electrochim. Sci.* 8 (2013) 3721–3730.
- [23] N.R. Manwar, R.G. Borkar, R. Khobragade, S.S. Rayalu, S.L. Jain, A.K. Banswal, N.K. Labhsetwar, Efficient solar photo-electrochemical hydrogen generation using nanocrystalline CeFeO₃ synthesized by a modified microwave assisted method, *Int. J. Hydrogen Energy* 42 (2017) 10931–10942.
- [24] Y. Wei, L.T. Kong, R. Yang, L. Wang, J.H. Liu, X.J. Huang, Electrochemical impedance determination of polychlorinated biphenyl using a pyrenecyclodextrin-decorated single-walled carbon nanotube hybrid, *Chem. Commun.* 47 (2011) 5340–5342.
- [25] R.X. Xu, X.Y. Yu, C. Gao, Y.J. Jiang, D.D. Han, J.H. Liu, X.J. Huang, Non-conductive nanomaterial enhanced electrochemical response in stripping voltammetry: the use of nanostructured magnesium silicate hollow spheres for heavy metal ions detection, *Anal. Chim. Acta* 790 (2013) 31–38.
- [26] N. Promphet, P. Rattanarat, R. Rangkupan, O. Chailapakul, N. Rodthongkum, An electrochemical sensor based on graphene/polyaniline/polystyrene nanoporous fibers modified electrode for simultaneous determination of lead and cadmium, *Sensor. Actuator. B Chem.* 207 (2015) 526–534.
- [27] Y. Chu, F. Gao, F. Gao, Q. Wang, Enhanced stripping voltammetric response of Hg²⁺, Cu²⁺, Pb²⁺ and Cd²⁺ by ZIF-8 and its electrochemical analytical application, *J. Electroanal. Chem.* 835 (2019) 293–300.
- [28] E.P. Randviir, A cross examination of electron transfer rate constants for carbon screen-printed electrodes using Electrochemical Impedance Spectroscopy and cyclic voltammetry, *Electrochim. Acta* 286 (2018) 179–186.
- [29] T. Holm, S. Sunde, F. Seland, D.A. Harrington, Understanding Reaction Mechanisms Using Dynamic Electrochemical Impedance Spectroscopy: Methanol Oxidation on Pt, *Electrochimica Acta*, 2019.
- [30] S. Dehdashtian, M. Shamsipur, Modification of gold surface by electro-synthesized monoaza crown ether substituted catechol-terminated alkane diithiol and its application as a new electrochemical sensor for trace detection of cadmium ions, *Colloids Surf. B Biointerfaces* 171 (2018) 494–500.
- [31] K. Kim, J.W. Han, Mechanistic study for enhanced CO oxidation activity on (Mn, Fe) co-doped CeO₂ (111), *Catal. Today* 293–294 (2017) 82–88.
- [32] G.H. Hwang, W.K. Han, J.S. Park, S.G. Kang, Determination of trace metals by anodic stripping voltammetry using a bismuth-modified carbon nanotube electrode, *Talanta* 76 (2008) 301–308.
- [33] Y.-F. Sun, W.-K. Chen, W.-J. Li, T.-J. Jiang, J.-H. Liu, Z.-G. Liu, Selective detection toward Cd²⁺ using Fe₃O₄/RGO nanoparticle modified glassy carbon electrode, *J. Electroanal. Chem.* 714–715 (2014) 97–102.
- [34] A. Afkhami, R. Moosavi, T. Madrakian, H. Keypour, A. Ramezani-Aktij, M. Mirzaei-Monsef, Construction and application of an electrochemical sensor for simultaneous determination of Cd(II), Cu(II) and Hg(II) in water and foodstuff samples, *Electroanalysis* 26 (2014) 786–795.
- [35] X. Chen, Z.G. Liu, Z.Q. Zhao, J.H. Liu, X.J. Huang, SnO₂ tube-in-tube nanostructures: Cu@C nanocable templated synthesis and their mutual interferences between heavy metal ions revealed by stripping voltammetry, *Small* 9 (2013) 2233–2239.
- [36] T. Zhang, H. Jin, Y. Fang, J. Guan, S. Ma, Y. Pan, M. Zhang, H. Zhu, X. Liu, M. Du, Detection of trace Cd²⁺, Pb²⁺ and Cu²⁺ ions via porous activated carbon supported palladium nanoparticles modified electrodes using SWASV, *Mater. Chem. Phys.* 225 (2019) 433–442.
- [37] S.-F. Zhou, X.-J. Han, Y.-Q. Liu, SWASV performance toward heavy metal ions based on a high-activity and simple magnetic chitosan sensing nanomaterials, *J. Alloys Compd.* 684 (2016) 1–7.
- [38] W.-J. Li, X.-Z. Yao, Z. Guo, J.-H. Liu, X.-J. Huang, Fe₃O₄ with novel nanoplate-stacked structure: surfactant-free hydrothermal synthesis and application in detection of heavy metal ions, *J. Electroanal. Chem.* 749 (2015) 75–82.
- [39] S. Duan, Y. Huang, Electrochemical sensor using NH₂-MIL-88(Fe)-rGO composite for trace Cd²⁺, Pb²⁺, and Cu²⁺ detection, *J. Electroanal. Chem.* 807 (2017) 253–260.
- [40] A. Shah, S. Sultan, A. Zahid, S. Aftab, J. Nisar, S. Nayab, R. Qureshi, G.S. Khan, H. Hussain, S.A. Ozkan, Highly sensitive and selective electrochemical sensor for the trace level detection of mercury and cadmium, *Electrochim. Acta* 258 (2017) 1397–1403.
- [41] G. Bhanjana, N. Dilbaghi, R. Kumar, A. Umar, S. Kumar, SnO₂ quantum dots as novel platform for electrochemical sensing of cadmium, *Electrochim. Acta* 169 (2015) 97–102.
- [42] C.H. Lin, P.H. Li, M. Yang, J.J. Ye, X.J. Huang, Metal replacement causing interference in stripping analysis of multiple heavy metal analytes: kinetic study on Cd(II) and Cu(II) electroanalysis via experiment and simulation, *Anal. Chem.* 91 (2019) 9978–9985.
- [43] S.-F. Zhou, J.-J. Wang, L. Gan, X.-J. Han, H.-L. Fan, L.-Y. Mei, J. Huang, Y.-Q. Liu, Individual and simultaneous electrochemical detection toward heavy metal ions based on L-cysteine modified mesoporous MnFe₂O₄ nanocrystal clusters, *J. Alloys Compd.* 721 (2017) 492–500.
- [44] A. Mardegan, P. Scopece, F. Lambertini, M. Meneghetti, L.M. Moretto, P. Ugo, Electroanalysis of trace inorganic arsenic with gold nanoelectrode ensembles, *Electroanalysis* 24 (2012) 798–806.